Cent. Eur. J. Phys. • 9(4) • 2011 • 956-961
DOI: 10.2478/s11534-010-0117-6

VERSITA

Central European Journal of **Physics**

Time-dependent wave packet theoretical study of femtosecond photoelectron spectra and coupling between the $A^2\Sigma^+$ and $B^2\Pi$ states of the NO molecule in a strong laser field

Research Article

Yonghua Zhu[1], Peng Song[1], Huan Yang[2*], Fengcai Ma[1†]

1 *Department of Physics, Liaoning University, Shenyang, P. R. China*

2 *School of Physics, Shandong University, Jinan, P. R. China*

Received 2 August 2010; accepted 25 October 2010

Abstract: In this work, the femtosecond time-resolved photoelectron spectra and the coupling between the $A^2\Sigma^+$ and $B^2\Pi$ states of the NO molecule in a strong laser field have been investigated by the time-dependent wave packet method. We demonstrate that the weak coupling between the $A^2\Sigma^+$ and $B^2\Pi$ states of NO plays a key role on the peak centered at 0.37 eV of the photoelectron spectra in the 2+1' channel.

PACS (2008): 32.80.Aa, 32.80.Fb, 32.80.Qk

Keywords: strong field • photoelectron spectrum • wave packet • femtochemistry

1. Introduction

Femtosecond laser technology has been widely applied in the fields of physics and chemistry [1–4]. In the past decade, a number of interesting phenomena in the intense femtosecond laser field, such as above threshold ionization (ATI) [5, 6], AC-Stark shift [7–9], harmonic generation [10, 11], coherent phenomena [12, 13], and laser-induced continuum structure [14], have been reported. Recently, control of chemical reaction has become a hot topic in femtochemistry [15, 16].

As we know, NO has been studied theoretically and experimentally as one of the most important di-atomic molecules owing to its significance in atmospheric pollution and atmospheric chemistry. The ultrafast dynamics of NO in a femtosecond laser field has been investigated experimentally and theoretically [17–29]. In 1996, Ludowise et al. obtained the femtosecond time-resolved photoelectronic spectrum (PES) of NO by use of (2+1') multi-photon ionization (MPI) in strong laser fields (pump at 380 nm, probe at 253 nm). In 2003, Han and coworkers used the time-dependent wave-packet dynamics method to calculate the femtosecond PES. As a result, they de-

*E-mail: hyangsdu@126.com (Corresponding author)
†E-mail: fcma@lnu.edu.cn

termined the effect of laser fields on the NO interaction potentials, and interpreted the phenomena of the potential shifting, and the coupling strength between the $C^2\Pi$ and $B^2\Pi$ states changing, as being caused by "trapped" molecules. Recently, Wang et al. utilized a femtosecond time-resolved velocity map imaging method combined with multi-photon ionization to study the optical field modulation of NO Rydberg state populations [29].

In the experiment [29] two femtosecond pulses referred to as the pump pulse and the probe pulse, were employed. The NO was excited from its ground state ($X^2\Sigma^+$) to a low-lying excited state ($A^2\Sigma^+$ or $C^2\Pi$) by the pump pulse. The probe pulse subsequently provided enough energy for the excited NO molecule to transition to the ionic state ($X^1\Sigma^+$). Wang et al. assigned two peaks centered at 0.82 and 2.35 eV as the 2+1′ and 2+2 multi-photon ionizations, which are excited to $A^2\Sigma^+$ by one-color photons (pump at 408 nm). In the overlap region of the pump and probe lights, the 0.37 eV peak was observed when the intensity of the pump laser was higher than 2.9×10^{12} W/cm^2, which indicates that the Rydberg-valance coupling between the $A^2\Sigma^+$ and $B^2\Pi$ states is a important factor.

In this work, the femtosecond PES of NO via 2+1′ MPI (pump at 408 nm, probe at 271 nm) has been calculated and compared with the experimental results. In our time-dependent wave-packet dynamics calculation, four states (the ground state of the NO molecule: $X^2\Pi$, the two excited states of the NO molecule: $A^2\Sigma^+$ and $B^2\Pi$, and the ground electronic state of the NO ion: $X^1\Sigma^+$) were used. In the following parts, we will use X, A, B, and I to denote $X^2\Pi$, $A^2\Sigma^+$, $B^2\Pi$, and $X^1\Sigma^+$ states, respectively. The potential curves of the NO molecule and the NO ion are shown in Figure 1.

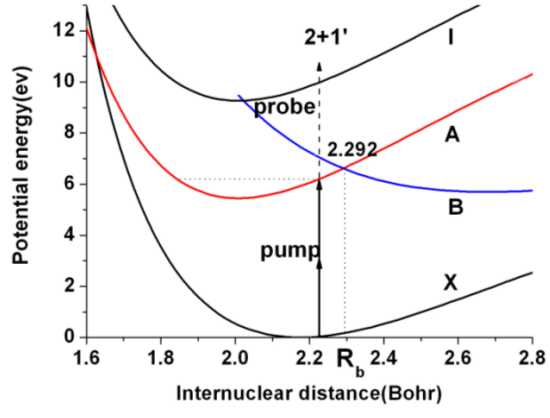

Figure 1. The NO potential curves employed in our calculation [20–24, 29]

2. Theoretical method

The time-dependent wave-packet dynamics method has been developed by Han and coworkers to widely study the non-adiabatic processes and femtosecond ultrafast dynamics [21–24, 32–35]. Invoking the Born-Oppenheimer approximation and neglecting the coupling between the core and the photoelectron, we can write the Hamiltonian for the vibrational motion of the NO molecule as:

$$H = -\frac{\hbar^2\partial^2}{2\mu\,\partial R^2} I + V(R,t), \tag{1}$$

where I is the identity matrix, R is the inter-nuclear separation, and μ is the reduced mass of the NO molecule, while the potential matrix $V(R,t)$ for 2+1′ in Eq. (1) can be explicitly written as:

$$V(R,t) = \begin{pmatrix} V_X & V_{XA} & 0 & \cdots & \cdots & 0 \\ V_{AX} & V_A & V_{AB} & V_{AI} & \cdots & V_{AI} \\ 0 & V_{BA} & V_B & \cdots & \cdots & 0 \\ \vdots & V_{AI} & \vdots & V_I + E_{I,1} & \cdots & \vdots \\ \vdots & \vdots & \vdots & \vdots & \ddots & 0 \\ \vdots & V_{AI} & 0 & \cdots & 0 & V_I + E_{I,1} \end{pmatrix}, \tag{2}$$

where the subscripts X, A, B and I represent the ground state of the NO, the excited states of the NO and the electronic state of the NO ion, respectively, and V_J (J = X, A, B) refer to the potential energies of the ground state $X^2\Pi$ and the excited states $A^2\Sigma^+$ and $B^2\Pi$ of the NO molecule. Here V_I can be designated as the potential energy of electronic state $X^1\Sigma^+$ of the NO ion. For a given electronic state of the NO ion, the free electron-ion pair states are described by 40 discrete states. $V_I + E_{I,n}$, $(n = 1, 2, \ldots, 40)$, denote the total energies of the discrete set of continuum states in the part of the free electron, and $E_{I,n}$, $(n = 1, 2, \ldots, 40)$ are the electron kinetic energies for one of the free electronic states of the NO ion. V_{ij} denotes the coupling between the ground state or the excited state $A^2\Sigma^+$ of the NO molecule and the electronic state of the NO ion, which can be written as:

$$V_{ij} = V_{ji} = \mu_{ij}\cdot E(t),\ (i,j = \mathrm{X, A, J}), \tag{3}$$

where μ_{ij} and $E(t)$ are the dipole matrix elements and the external field, respectively. The dipole matrix element μ_{XA} between the ground state $X^2\Pi$ and the excited state $A^2\Sigma^+$ is assumed to be a function of the internuclear distances [21]. The coupling strengths between bound states and continuum states are much smaller than those between

bound states, which are considered to be about a factor of 10 lower than the coupling strengths between the ground and excited states [30, 31]. In our calculation, the coupling between ground state and continuum states is omitted. The interaction potential V_{AB} (AB coupling), varying with R, takes the form of a Gaussian function, which is similar to the BC coupling [21]:

$$V_{AB} = V \times \exp\left(-\frac{(R-R_b)^2}{\beta^2}\right), \tag{4}$$

where V is the coupling amplitude of the A and B states, R_b the coupling center position (see Fig. 1) and β the coupling width. According to the transition rule, coupling between the ground state or ionic states and the $B^2\Pi$ state is forbidden and can be set to 0. The shape of the laser pulse is chosen as:

$$E(t) = \sqrt{\frac{8\pi I}{c}} f(t)\cos\omega t, \tag{5}$$

where

$$f(t) = \exp\left(-\frac{(t-t_0)^2}{2\sigma^2}\right)$$

is the pulse envelope function, I the laser intensity, c the velocity of light in vacuum, t_0 the central value of the pulse, ω the central frequency, and σ is relevant to the laser full width at half maximum. The time-dependent Schrödinger equation is solved by the "split-operator-Fourier" method [21–24, 32–35]. The evolution of the wave packets with time can be expressed as:

$$\Psi(R, t+\triangle t) \approx U_T^{\frac{1}{2}}(R, t+\triangle t) U_V U_T^{\frac{1}{2}}(R, t+\triangle t)\Psi(R, t), \tag{6}$$

where U_T and U_V denote the kinetic and potential energy evolution operators, respectively. The kinetic energy operator is given by:

$$U_T = \exp\left(-\frac{i\triangle t}{\hbar} T_R\right) = F^{-1}\exp\left(-\frac{i\hbar k^2 \triangle t}{2\mu}\right) F, \tag{7}$$

where F denotes the Fourier transform

$$F(t) = \frac{1}{\sqrt{2\pi}}\int_{-\infty}^{\infty} dR' \exp\left(ikR'\right) f\left(R'\right). \tag{8}$$

The potential operator is calculated by:

$$\begin{aligned} U_V &= \exp\left(-\frac{i\lambda\triangle t}{\hbar} V\right) \\ &= M\exp\left(-\frac{i\lambda\triangle t}{\hbar} M^T V M \triangle t\right) M^T \\ &\quad M\left(\begin{bmatrix} \exp\left(-\frac{i\lambda_1\triangle t}{\hbar} V\right) & \cdots & 0 \\ \vdots & \ddots & \vdots \\ 0 & \cdots & \exp\left(-\frac{i\lambda_n\triangle t}{\hbar} V\right) \end{bmatrix}\right) M^T, \end{aligned} \tag{9}$$

where M denotes the matrix that diagonalizes the potential matrix V from Eq. (2), the superscript T represents the transpose of the matrix, and $\lambda_1, \lambda_2, \ldots, \lambda_n$ are the eigenvalues of the matrix V. Therefore, Eq. (6) can be rewritten as:

$$\begin{aligned} &\Psi(R, t+n\triangle t) \\ &\quad \approx \prod_{k=0}^{n-1}(R, t+k\triangle t) U_V U_T^{\frac{1}{2}}(R, t+k\triangle t)\Psi(R, t). \end{aligned} \tag{10}$$

In this study, the time internal $\triangle t = 0.2$ fs was found to be suitable for convergent results. The parameters, such as laser wavelengths, beam width and intensity, are the same as those of the experiment [29], with the exception of the AB coupling (adjustable parameter).

3. Results and discussion

The femtosecond time-resolved photoelectron spectra from 2+1′ MPI of NO at fixed pump (408 nm) and probe (271 nm) wavelengths for a pump-probe delay time of 0 fs are calculated and shown in Fig. 2. The pump intensities are 1.9×10^{12} W/cm^2, 2.9×10^{12} W/cm^2, 5.7×10^{12} W/cm^2 and 23.0×10^{12} W/cm^2 in Fig. 2a-2d, respectively. The probe intensity is 5.7×10^{11} W/cm^2 for all the above cases. From Fig. 2, we can clearly see that though the peak b at 0.82 eV exists for all pump intensities, the peak g at 0.37 eV increases with pump laser intensity. It should be noted that the coupling between A and B has to be considered in our calculations. If the coupling is neglected, only peak b, centered at 0.82 eV, remains. Returning to Eq. (4), if we assume V and R_b are constants, we find that β increases with the pump laser intensity, which is in accordance with the experimental results. This indicates that the range of the coupling space between A and B expands with pump laser intensity.

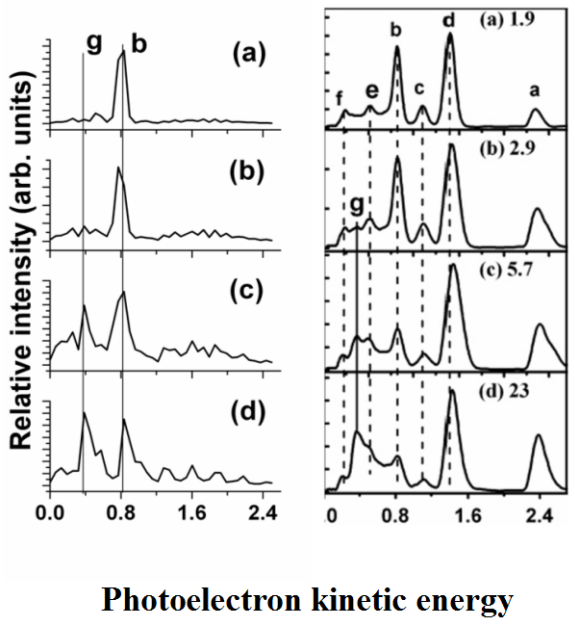

Figure 2. The results of the calculation (left) and experiment (right) of the femtosecond time-resolved photoelectron spectra from 2+1' MPI of NO at fixed pump (408 nm) and probe (271 nm) wavelengths for a pump-probe delay time of 0 fs for several pump intensities. (a)-(d) correspond to the pump laser intensities 1.9×10^{12} W/cm^2, 2.9×10^{12} W/cm^2, 5.7×10^{12} W/cm^2 and 23.0×10^{12} W/cm^2, respectively. The peaks b and g in the experimental data are at 0.82 eV and 0.37 eV, respectively. The thin lines g and b in the calculation results represent the positions of the peaks at 0.37 eV and 0.82 eV of the experiment [29], respectively.

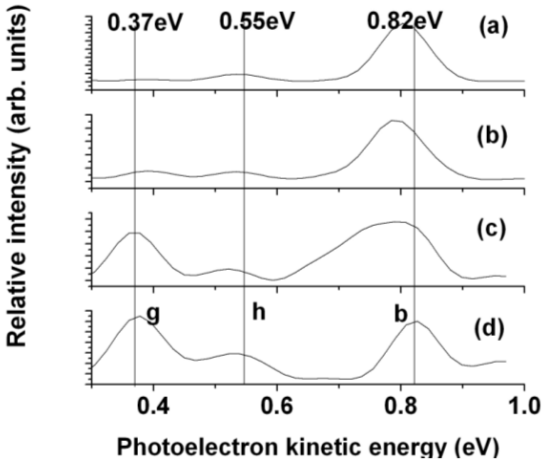

Figure 3. Part of the femtosecond time-resolved photoelectron spectra in Fig. 2, ranging from 0.3 to 1.0 eV. The new 0.55 eV peak h, which wasn't explained by the 2+1' channel in the experiment [29], appears in our calculations and is marked.

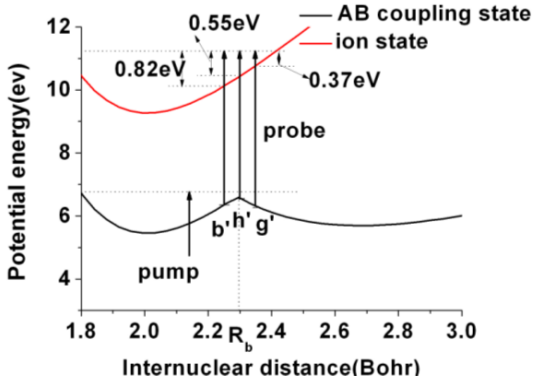

Figure 4. Potential line of the AB coupled state. The letters g', h' and b' represent three vibrational states of the coupled excited state.

In Fig. 2a, the peak b is dominant, while the peak g is too weak to be observed. As the pump intensity increases to 2.9×10^{12} W/cm^2, as shown in Fig. 2b, the peak g is still weak but can be resolved from the other small peaks. With further increases of the pump intensity, the peak g becomes as clear as peak b in Fig. 2c and even stronger than peak b in Fig. 2d. The results 2a-2d are consistent with those of the experiment [29]. To improve the resolution of the investigation, the energy range from 0.3 to 1.0 eV is selected and the calculated results are shown in Fig. 3a-3d. From Fig. 3, a new peak h, centered at 0.55 eV, is observed to increase with the pump intensity. It is thought to be mixed with the peak e in Ref. [29] of the photoelectron spectra of the 1'+2 channel, which cannot be distinguished from the peak e in the experiment. By the above analysis, we conclude that peak b resulted from the A state, since the peaks g and h appear only when the AB coupling is considered. The three peaks in Fig. 3 can be explained clearly by Fig. 4. Following pumping, the wave packet is excited to the A state. However due to the AB coupling, a new coupled excited state is formed, which is shown as the black line in Fig. 4. The characters b', h' and g' represent the three different vibrational states, respectively. The probe pulse causes ionization from the vibrational states to the ionic state resulting in three different electron energies (0.82, 0.55 and 0.37 eV), which correspond to peaks b, h and g, respectively. Furthermore, we can explain the dependence of the three different peaks on the pump intensity.

1. If the AB coupling is neglected, only the peak b exists, that is to say, only the transition between the b′ vibrational level and ionic state occurs.

2. When the pump intensity is weak, the coupling width is small. Since the h′ vibrational level is near to the position (see Fig. 4), it is affected most and the transition between the h′ vibrational state and ionic state can occur. As a result, the transition between b′ and ionic state dominates and the transition from h′ is weak.

3. The stronger the pump intensity is, the larger is. When is large enough, the b′ and g′ vibrational levels are both affected. The probability of the transition between the g′ vibrational level and ionic state increases, while that of the b′ transition decreases.

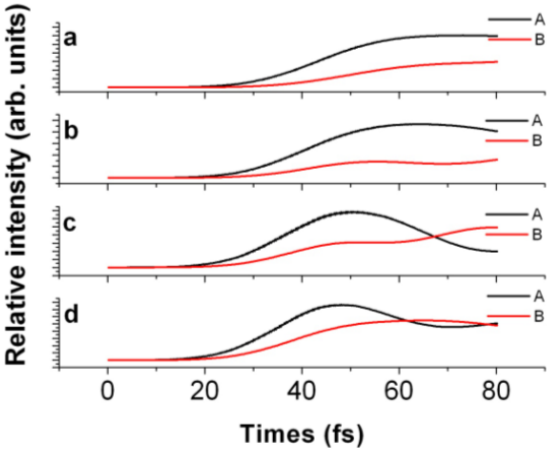

Figure 5. The populations of the A and B states with the evolution of time at different pump intensities. (a)-(d) correspond to the pump laser intensities 1.9×10^{12} W/cm^2, 2.9×10^{12} W/cm^2, 5.7×10^{12} W/cm^2 and 23.0×10^{12} W/cm^2, respectively, for a pump-probe delay of 0 fs.

The effect of a strong field on the coupling can also be illustrated by the population of the A and B states during the interaction between thepump and probe fields and NO, as shown in Fig. 5. If this coupling is neglected, the population of the B state is zero. As we can see from Fig. 5, as the result of the interaction of the pump pulse, the population of the B state increases. With increasing pump intensity, the population of the B state increases quickly to a high level in a short time. In other words, the B state has a large population for a long time. The probe pulse increases the probability of the transition from the B state to the ionic state. We can conclude that the coupling between the A and B states becomes stronger with increasing pump laser intensity, which is consistent with the above statement.

4. Conclusion

In this paper, an accurate quantum mechanical method was employed to calculate part of the photoelectron spectrum of the NO molecule (2+1′ MPI). By using the coupling between A and B states, the peak g was explained. The coupling between the A and B states varying with R takes the form of a Gaussian function, similarly to the BC coupling. The coupling amplitude and center position are constant, and the coupling width increases with the pump laser intensity. The effect of a strong field on coupling was also illustrated by the populations of the A and B states during the interaction between the laser fields and NO species.

The other peaks (c, d, e, f) resulting from the 1′+2 channel of the experiment [29] were not studied in the present work. More complete studies of the full photoelectron energy spectra are planned for future investigation.

Acknowledgments

The experimental data was supplied by B.X. Wang and we thank him for his helpful discussion. The code used in our calculation was provided by Professor K.L. Han and we appreciate his help and kind advice.

References

[1] T.S. Chu, Y. Zhang, K.L. Han, Int. Rev. Phys. Chem. 25, 201 (2006)
[2] J. Hu, K.L. Han, G.Z. He, Phys. Rev. Lett. 95, 123001 (2005)
[3] K.L. Han, G.Z. He, J. Photoch. Photobio. C 8, 55 (2007)
[4] G.J. Zhao, K.L. Han, Y.B. Lei, Y.S. Dou, J. Chem. Phys. 127, 094307 (2007)
[5] M. Busuladzic, A. Gazibegovic-Busuladzic, D.B. Milosevic, W. Becker, Phys. Rev. Lett. 100, 203003 (2008)
[6] E.R. Peterson, P.H. Bucksbaum, Phys. Rev. A 64, 053405 (2001)
[7] C.P. Liu, T. Nakajima, T. Sakka, H. Ohgaki, Phys. Rev. A 77, 043411 (2008)
[8] Y. Xiang, Y.P. Niu, S.Q. Gong, Phys. Rev. A 80, 023423 (2009)

[9] C.P. Liu, T. Nakajima, Phys. Rev. A 78, 063424 (2008)
[10] P. Tzankov et al., Opt. Express 15, 6389 (2007)
[11] I.V. Hertel, W. Radloff, Rep. Prog. Phys. 69, 1897 (2006)
[12] J.K.L. Knappenberger, E.B.W. Lerch, P. Wen, S.R. Leone, J. Chem. Phys. 125, 174314 (2006)
[13] M. Wollenhaupt, V. Engel, T. Baumert, Annu. Rev. Phys. Chem. 56, 25 (2005)
[14] O. Faucher et al., J. Phys. B: At. Mol. Opt. Phys. 32, 4485 (1999)
[15] T.P. Rakitzis, A.J. van den Brom, M.H.M. Janssen, Science 303, 1852 (2004)
[16] M. Wollenhaupt, V. Engel, T. Baumert, Annu. Rev. Phys. Chem. 56, 25 (2005)
[17] T. Dove, T.W. Schmidt, R.B. Lopez-Martens, G. Roberts, Chem. Phys. 267, 115 (2001)
[18] R.B. Lopez-Martens, T.W. Schmidt, G. Roberts, Phys. Rev. A 62, 013414 (2000)
[19] T.W. Schmidt, R.B. Lopez-Martens, G. Roberts, J. Phys. B: At. Mol. Opt. Phys. 37, 1125 (2004)
[20] P. Ludowise, M. Blackwell, Y. Chen, Chem. Phys. Lett. 258, 530 (1996)
[21] Q.T. Meng, G.H. Yang, H.L. Sun, K.L. Han, N.Q. Lou, Phys. Rev. A 67, 063202 (2003)
[22] G.J. Zhao, Y.H. Liu, K.L. Han, Y. Dou, Chem. Phys. Lett. 453, 29 (2008)
[23] H. Zhang, K.L. Han, G.Z. He, N.Q. Lou, Chem. Phys. Lett. 289, 494 (1998)
[24] Y.H. Liu, G.J. Zhao, G.Y. Li, K.L. Han, J. Photoch. Photobio. A 209, 181 (2010)
[25] R. de Vivie, S.D. Peyerimhoff, J. Chem. Phys. 89, 3028 (1988)
[26] R. de Vivie, M.C. Hemert, S.D. Peyerimhoff, J. Chem. Phys. 92, 3613 (1990)
[27] K.P. Huber, G. Herzberg, Molecular spectra and molecular structure. IV. Constants of diatomic molecules (Van Nostrand Reinhold, New York, 1979)
[28] W. Guo, J.Y. Zhu, B.X. Wang, Y.Q. Wang, L. Wang, Chem. Phys. Lett. 448, 173 (2007)
[29] B.X. Wang, B.K. Liu, Y.Q. Wang, L. Wang, Phys. Rev. A 81, 043421 (2010)
[30] G.Y. Li, G.J. Zhao, Y.H. Liu, K.L. Han, G.Z. He, J. Comput. Chem. 31, 1759 (2010)
[31] C. Meier, V. Engel, Chem. Phys. Lett. 212, 691 (1993)
[32] T. Chen, W.P. Zhang, X. Wang, G.J. Zhao, Chem. Phys. 365, 158 (2009)
[33] T.S. Chu, K.L. Han, Phys. Chem. Chem. Phys. 10, 2431 (2008)
[34] T.X. Xie, Y. Zhang, M.Y. Zhao, K.L. Han, Phys. Chem. Chem. Phys. 5, 2034 (2003)
[35] K.L. Han, G.Z. He, N.Q. Lou, J. Chem. Phys. 105, 8699 (1996)